DESIGN AND ANALYSIS OF A 1 KW RANKINE POWER CYCLE, EMPLOYING A MULTI-VANE EXPANDER, FOR USE WITH A LOW TEMPERATURE SOLAR COLLECTOR

by

THOMAS ALAN DAVIDSON

Submitted in Partial Fulfillment
of the Requirements for the
Degree of Bachelor of Science
at the
MASSACHUSETTS INSTITUTE OF TECHNOLOGY
May, 1977

Signature of Author. . . . . .
Department of Mechanical Engineering May 12, 1977

Certified by. . . . . .
Thesis Supervisor

Accepted by. . . . . .
Chairman, Departmental Committee on Theses

DESIGN AND ANALYSIS OF A 1 KW RANKINE POWER CYCLE, EMPLOYING A MULTI-VANE EXPANDER, FOR USE WITH A LOW TEMPERATURE SOLAR COLLECTOR

by

THOMAS ALAN DAVIDSON

Submitted to the Department of Mechanical Engineering on May 12, 1977 in partial fulfillment of the requirements for the Degree of Bachelor of Science.

Abstract

A 1 kw Rankine power cycle, employing a multivane expnader, has been designed and constructed. The cycle will utilize a solar collector operating at 210°F as the boiler, and Refrigerant R-11 as the working fluid. The predicted efficiency of the expander is 20% of Rankine at 500 rpm and 30% at 1000 rpm. A cycle analysis is performed, and sizing of cycle components discussed. An experimental program, aimed at testing the cycle under simulated collector conditions, is outlined.

Carl R. Peterson, Associate Professor of Mechanical Engineering

Table of Contents

List of Figures and Tables

List of Variables

A heat exchanger surface area

c_v specific heat (of R-11$_{(1,86^{o}F.)}$)

D tube diameter

E_e efficiency of expander= W_e / H_{air}

F_1 leakage fraction of working fluid in the expander

F_f total frictional loss in expander

g_x 32.2 lbm-ft/lbf-sec^2

G mass flow rate of the working fluid (lbm/min)

G_m vapor mass flow rate/cross sectional area of flow path

Gr_x Grashof number

h enthalpy value of the working fluid (Btu/lbm)

h_i, h_o contact coefficients of heat transfer

ΔH_{air} enthalpy change of compressed air

k heat transfer constant

K_a heat transfer coefficient

m mass of working fluid (for ideal gas law eqn)

m mass flow rate of working fluid

m_v mass of the expander's vanes

N_u Nusselt number

P pressure (lbf/ft^2)

Pr Prandl number

Q heat transfer

Q_c heat transfer across the condenser

Q_e heat transfer across the evaporator

r mean radial position of expander's vanes

T temperature

T_c working gluid temperature (for heat transfer)

T_H highest temperature ($^\circ$R or $^\circ$K)

T_L lowest temperature ($^\circ$R or $^\circ$K)

T_w wall temperature (for heat transfer)

U overall heat transfer coefficient

v volume of the working fluid (ft^3)

v_r expander rotor velocity

v_o volume of the working fluid (ft^3)

W_{ip} power consumption of a 100% efficient pump

W_{net} amount of work available from enthalpy change of the working fluid

W_{pump} actual power consumption of feed pump

x_a metal thickness for heat transfer

y_o distance between heat exchanger fins

W_e expander output

β thermal coefficient of volume expansion

γ specific heat ratio = c_p/c_v

η_c Carnot efficiency

η_L maximum expander efficiency after leakage losses

η_r Rankine efficiency

η_c cycle efficiency = Q_e/W_e

μ_e the expander's vane/stator coefficient of friction

ν kinematic viscosity (ft^2/hr)

$\eta_{(T+f_p)}$ = cycle efficiency with feed pump included $= Q_e/(W_e - W_{pump})$

Acknowledgements

The number of people and groups I should acknowledge for either directly helping me, or providing invaluable moral and emotional support, is almost too long to mention. First, I would like to acknowledge the continuing support of the Clapp and Poliak Engineering Design Award Committee, without whose financial assistance the project never would have gotten off the ground. I would also like to acknowledge the generous support of the Gast Manufacturing Corporation, Benton Harbor, Mich., for modifying and lending us the the 16AM-1CC air motor, providing the nucleus from which the power cycle was designed and constructed. The information found in Figures 2,7, and 8 was provided by Gast. The financial support of SCORE, Inc., via their coordinating committee, has also been invaluable in financing the project.

Among the individuals I would like to thank for their help on a more technical level are Professor Carl Peterson, my thesis advisor, and Professor Jim Felske, faculty advisor for our SCORE team. I would also like to thank Robert J. Raymond of Thermo Electron Corp., for researching many references and providing many suggestions for cycle components, and Spurgeon Eckard of General Electric, for his suggestions concerning the cycle expander.

The help of the members of SCORE team #79, in terms

of helping to design and construct the power cycle, has been invaluable. I am also deeply indebted to my many friends in the SCORE, 249 Pearl St., 69 Chestnut St., and W20-415 gangs for continued emotional support. I never could have done it without you.

Last, but not least, I would like to thank my parents for giving me the opportunity to come here, and providing continued financial support through the years. For my sister, Amy, who has so graciously volunteered to type my final draft, I know of no words that can express my appreciation. Without her help, I would be taken off of the degree list today.

I would like to dedicate this thesis to my first nephew, Christopher Michael Carver, in hope that he'll turn out to be a good little kid. Best wishes Sue and Terry, things look pretty promising so far.

Introduction

The topic for this thesis evolves from work I have been doing for the 1976-77 Student Competition on Relavent Engineering (SCORE). The goal of this competition is to design and build a system capable of producing an electrical output varying from 0.5 to 1.4 kw, utilizing an alternative energy input. Our entry, a 1 kw Rankine power cycle utilizing a low temperature solar collector as the boiler, has been designed and constructed, but not yet tested. It is the purpose of my thesis to examine the power cycle and analyze it in terms of applicability for a solar energy application.

In deciding on the type of system to design and construct for our entry, two major questions had to be answered. These questions were:

(1) what type of energy input to use, and (2) what type of power system to use to convert this energy into electricity. Due to time, money, and technical restraints, the group decided to choose a dependable and easily built system, as opposed to an efficient one. A low temperature solar collector was chosen to provide the energy input, and a heat engine to convert the heat to electricity. The Rankine thermodynamic cycle was chosen as the heat engine cycle because of its widespread use and the commercial availability of cycle components.

For this thesis, the experimental setup of the 1 kw test cycle is first described, with some discussion of the reasons underlying the choice of working fluid and individual components. An outline of the proposed experimental plan is included. Analysis will consist primarily of examining the efficiency of the expander. Other system components will also be analysed, and a cycle analysis to predict cycle preformance will be performed. To conclude, suggestions will be made for continuation of research on the cycle.

Experimental Setup

The type of power cycle built for our entry is a Rankine cycle. This cycle has four major components, which are:

(1) a feed pump, which takes the condensed working fluid and pumps it up to operating pressure,

(2) a boiler, where the pressurized fluid is vaporized,

(3) an expander, where the working fluid expands and produces shaft power,

and (4) a condenser, where the fluid is condensed to liquid form.

A generator attached to the expander shaft produces electrical power. Figure 1 is a schematic of our test cycle.

Working Fluids

Before choosing and sizing cycle components, several fluids were examined for possible use as a working fluid, including low pressure steam, and refrigerants R-11, R-113, and R-114. A refrigerant was chosen because of relatively high operating pressures and ability to mix easily with lubricants when compared to steam. The choice of a refrigerant meant that a closed cycle was necessary to avoid loss of working fluid; sealing the system became a major consideration.

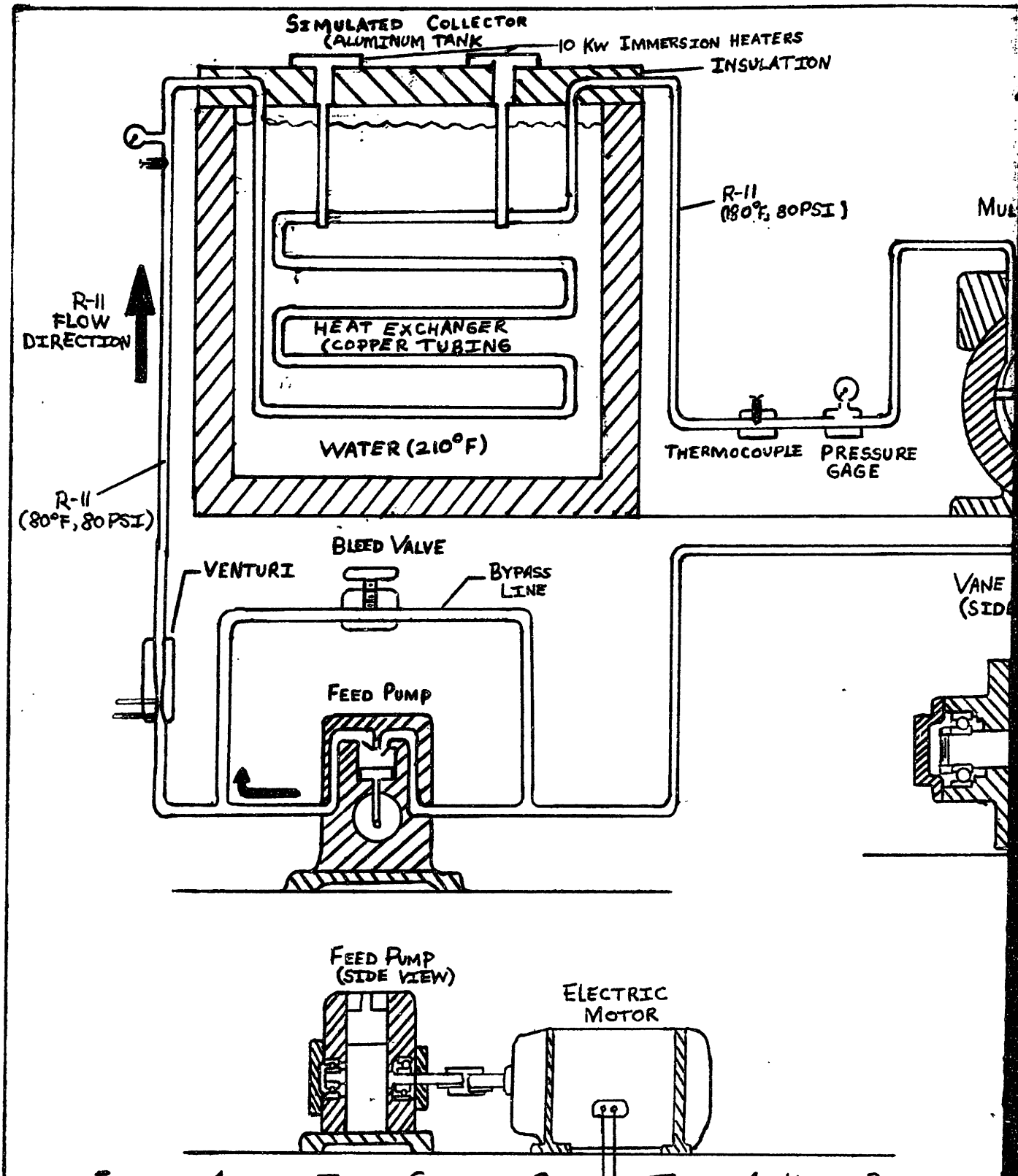

FIGURE 1 - TEST SETUP OF THE 1 KW RANKINE

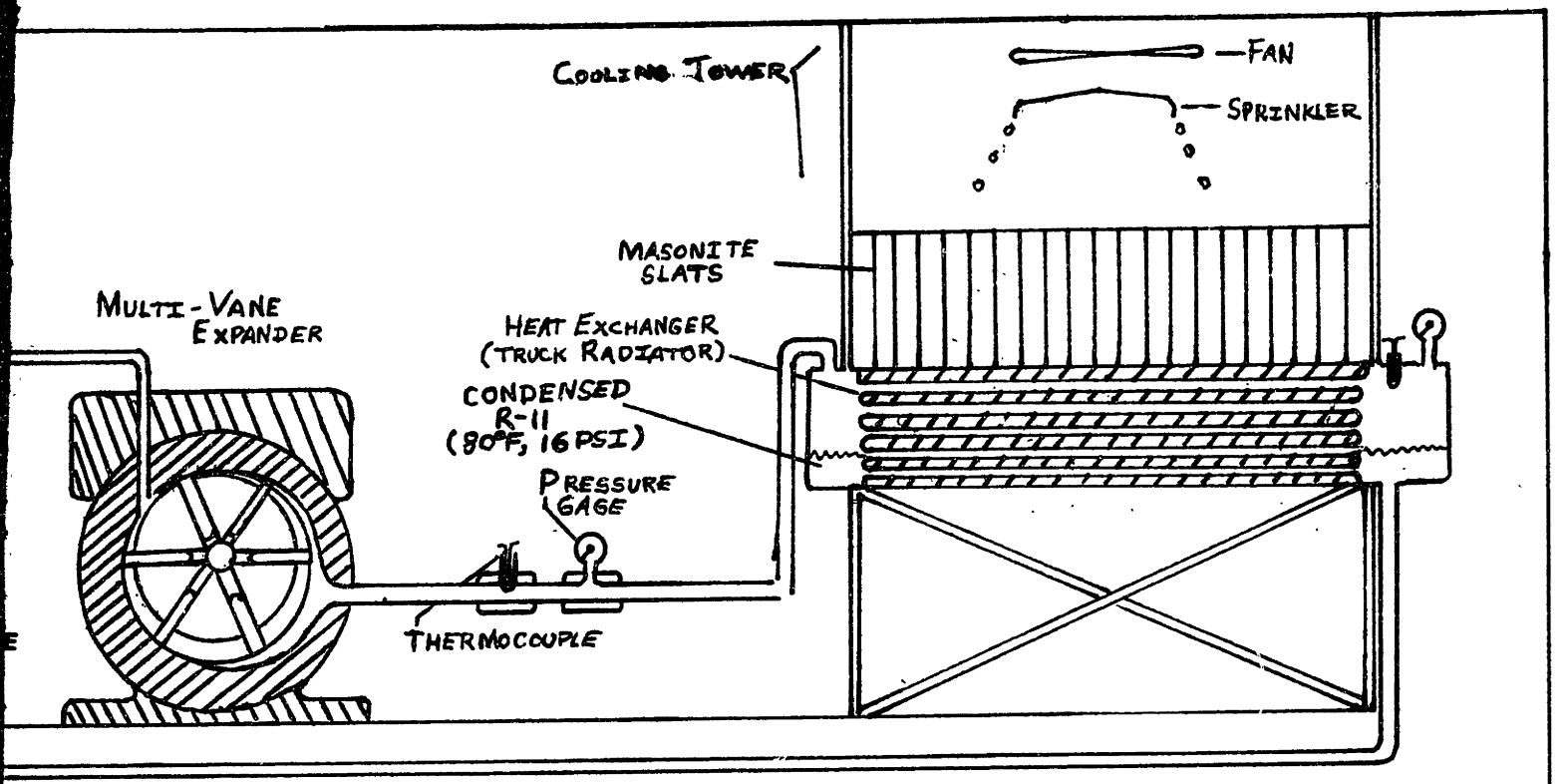

VANE EXPANDER (SIDE VIEW)

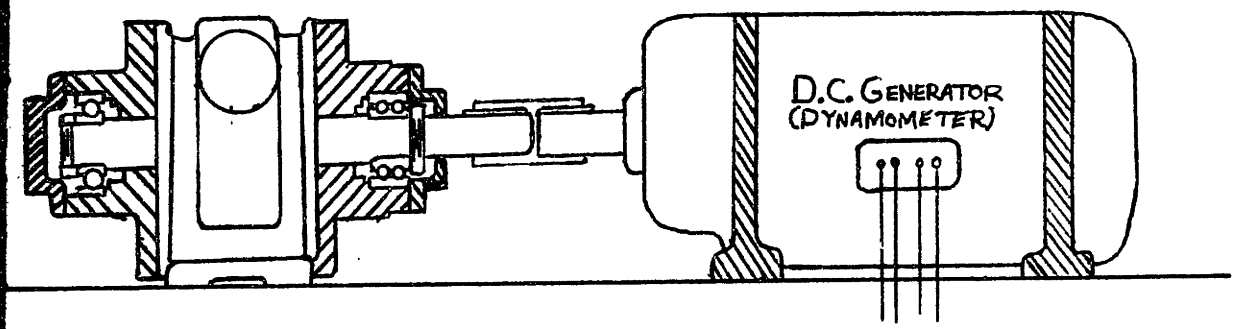

NKINE POWER CYCLE

Expander Alternatives

Four major alternatives have been considered for use as the expander. These alternatives are:

(1) a converted turbocharger operating at 10,000+ rpm,

(2) a very slow cycle (1 rpm), utilizing an approach similiar to Wally Minto's "Wonder Wheel"[9]

(3) the conversion of a reciprocating air conditioner compressor

and (4) the use of a modified multi-vane air motor. Turbochargers were ruled out when none were found of small enough size to work in this power range. Building a "Wonder Wheel" looked interesting, but was geared more towards a mechanical output than an electrical because of the low operating rpm. An air conditioning compressor sized to work in the speed range of 1800rpm was found and considered, but the construction of new valves for the compressor looked difficult, as did the problem of sealing. The fourth alternative, a multi-vane expander, looked most promising because of its simplicity of design, matching operating speeds, and availability. This alternative has been chosen.

The expander actually used for our cycle is a model 16AM-1CC air motor, manufactured by the Gast Mfg. Corp. This rotary-vane motor has a cast iron bore and six vanes. For our application, the expansion ratio of the motor has been changed from 2.0 to 2.65 by reducing the rotor diameter,

and modifying the inlet and exhaust ports. Figure 2 shows a cross section of the modified motor, as provided by Gast. The size of the motor made R-11 the best working fluid for obtaining a 1 kw output at 500 rpm. Spurgeon Eckard of General Electric, who has had considerable experience developing and testing multi-vane expanders for solar energy applications, felt that R-113 and R-114 would also be acceptable working fluids, but that R-113 would have higher inlet breathing losses, and R-114 would have higher internal leakage due to higher operating pressure. Eckard also made two additional suggestions for increasing the efficiency of this air motor; first, to remachine some of the internal components to improve surface finish and mating clearances, and second, to replace the vanes with a metal impregnated graphite material; such as Graphite grade CC-100, supplied by Carbone Corp. With these improvements, Eckard felt that the expander could achieve approximately 50% of Rankine efficiency at 500 rpm.[13]

Feed Pump

The feed pump we have chosen for our power cycle is a brass piston pump, manufactured by Hypro, with a 3.27 gpm flow rate at 1800 rpm. The sizing of this pump, and all other cycle components, was determined after the efficiency of the expander, and the corresponding mass and energy flow rates, were calculated. These calculations are made in Ap-

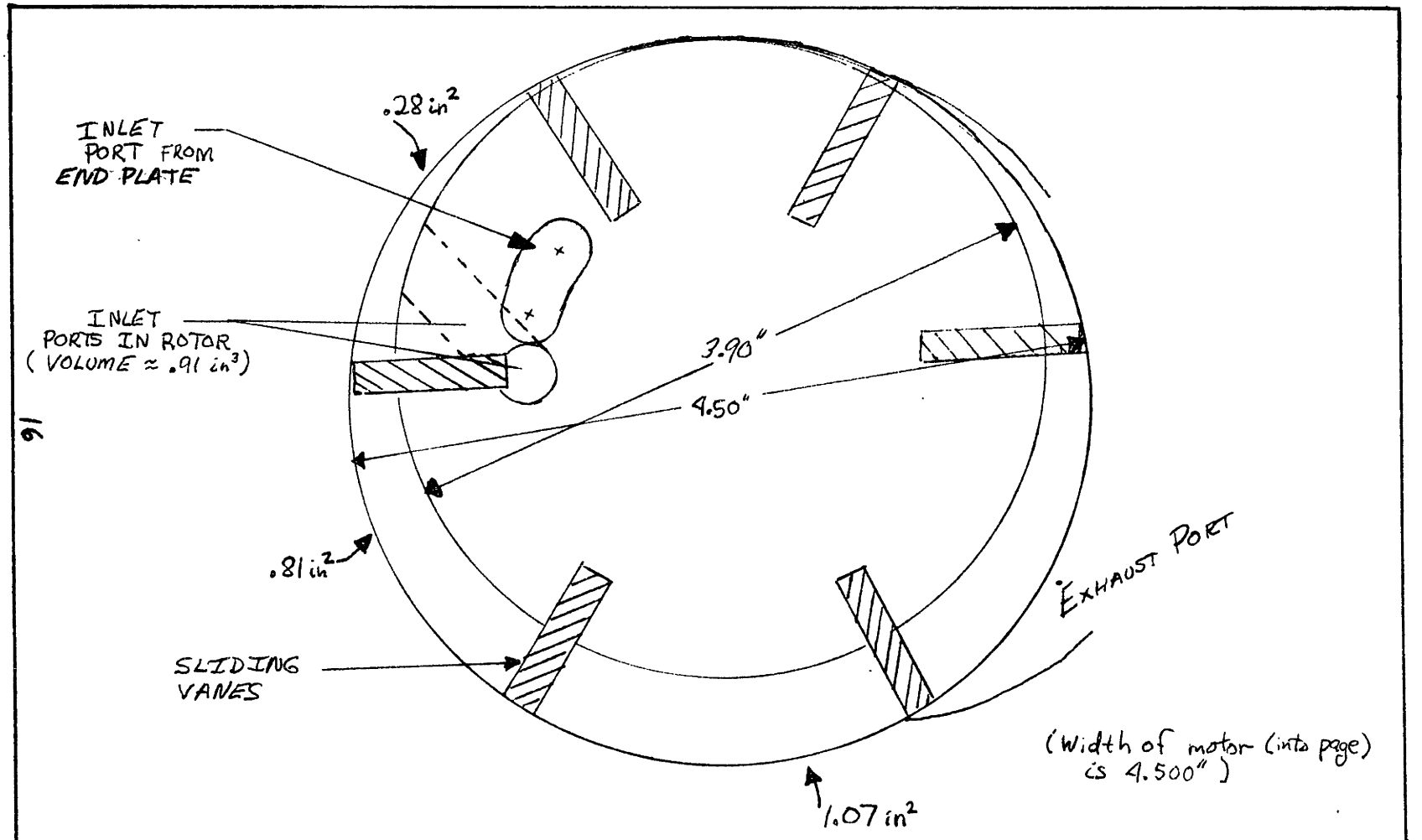

91

FIGURE 2 - CROSS SECTIONAL VIEW OF THE TEST EXPANDER

(COURTESY OF GAST MFG. CORP.)

pendices 1 and 3. The pump will be driven by a ½ Hp motor at 1725 rpm.

As we plan to test the efficiency of the expander over a range of speeds, it is desirable to vary the mass flow rate of the working fluid. Sufficient boiler heat exchange area exists to vaporize as much R-11 as is pumped into it, so, the mass and energy flow rates, and thus expander output are controlled by the amount of R-11 pumped. Original plans called for driving the pump with a variable speed motor, but one is not currently available, so, an expander bypass line controlled by a bleed valve has been inserted into the system in parallel with the feed pump. By opening and closing the bleed valve, the mass of working fluid circulating through the expander can be varied.

Condenser and Boiler

The condenser for the cycle is a modified copper truck radiator. This has been incorporated in a cooling tower; heat is removed as water evaporates from the fins of the radiator. The gross dimensions of the radiator are 30" by 27" by 4" deep. A total of 180 rectangular tubes, 1" by 3/16" OD (1/8" ID), run the 30" length of the radiator. The freon will condense primarily within these tubes. Copper fins, .005 inch thick and spaced .11 inch apart, run perpendicular to the tubes to increase the surface area exposed to the cooling tower water. The total surface area

of the rectangular tubes is 75 ft^2; that of the fins is 210 ft^2. The total surface area exposed to the cooling water is therefore 210+75=285 ft^2. The inner cross sectional area of each tube is approximately 1" x .125" = .125 in^2. The total cross sectional area of all 180 tubes is therefore (.125 in^2 x 180 = 22.5 in^2 = .156 ft^2. As calculated in Appendix 5, this size radiator is sufficient to reject 50 kw with a temperature differential of 33°F across the radiator.

The boiler, or simulated collector for the cycle, is 200 ft of ⅜" copper refrigeration tubing immersed in water in a $(3.5\ ft)^3$ insulated aluminum tank. The water can be heated to 210°F by two 10 kw immersion heaters. As calculated in Appendix 4, this length of copper tubing is sufficient to transfer 52 kw to the R-11 with a 36°F temperature differential across the tubing.

Potential Problems-rusting, sealing, and mixing

Several potential problems had to be investigated in using R-11 in a system where some components were not designed to work with this fluid. The problems I felt most worthy of investigation were:

(1) possible rusting of the cast iron bore of the air motor,

(2) the ability of the air motor and feed pump seals to withstand R-11 at 80 psi and 200°F,

and (3) the ability of a lubricant to mix with the R-11

and distribute itself to components in the cycle.

Using a refrigeration repairman as a source, I discovered that the probability of rusting is very large if any significant amount of water vapor is present in the cycle. To purge the water vapor from the cycle, a vacuum will be first drawn on the system. Nitrogen will then be introduced to diffuse remaining water vapor, and another vacuum of 100 microns has been recommended.[14]

From his experience, Eckard suggests mixing 3% refrigerant oil with the working fluid to keep components lubricated.[4] A potential problem is that without an oil-return line the oil may either (1) collect on top of the condensing refrigerant and never reach the feed pump, or (2) collect on the surface of the evaporating refrigerant, and not vaporize with it. R-11, however, mixes moderately well with refrigerant oils; it is often used to clean refrigeration systems.[14] Suniso 3g refrigerant oil will be used to lubricate the system.

To test the compatability of the air motor and feed pump seals with the working fluid, extra seals were ordered from both Gast and Hypro. The air motor seal material is Nitrile; very compatable with R-12 based on manufacturer's information. For the feed pump, both Buna-N and Teflon piston seals were available. While Teflon is the more compatable of the two materials, this seal leaks during the

early stages of use, so for limited testing the Buna-N seal has been chosen. To determine reasonable compatability, the seals were bathed in R-11 at 80°F for 2 weeks. Both seals were compatable by this test.

Instrumentation

To analyse system and component performance, the temperature and pressure of R-11 is measured before and after each component. Pressure gages are used for the pressure measurement; thermocouples for the temperature. The output of the thermocouples is read by a voltmeter. Working fluid flow rate will be measured by a Barco Model #402 venturi placed in the system just before the fluid enters the boiler. A differential pressure transducer will be attached to the venturi, and its output will be measured by a voltmeter. Expander speed will be measured by a stroboscope. Power output will be determined by measuring the output of a 3/4 Hp D.C. generator attached to a resistance load. The D.C. generator will be pre-calibrated to determine its efficiency at the speeds and field strengths to be used during experimentation.

Experimental Program

Due to variable solar insolation, the temperature of our collector, as well as the amount of heat that can be drawn from it at constant temperature, will vary with time of day and time of year. To be applicable for a solar energy

application, therefore, a power cycle must be able to operate over a range of collector temperatures, and also over a range of power outputs, with fair efficiency. An experimental program, aimed at testing this cycle efficiency, is outlined below.

Three variables that need to be controlled for testing are:

(1) the simulated collector temperature

(2) the temperature of the condensing water

and (3) the mass flow rate of R-11.

The collector is designed to operate between 180°F and 210°F, the condensing water temperature between 50°F and 70°F, and the mass flow rate of R-11 from 25 lbs/min to 35 lbs/min, depending on desired power output and collector temperature. To test the expander, system measurements could be taken for the following values of the controllable variables:

(1) simulated collector temperature-180°F to 210°F, at 5°F intervals

(2) condensing water temperature-50°F, 60°F, 70°F

(3) R-11 mass flow rate-25, 30, and 35 lbs/min.

If data is taken for all the above combinations, there will be a total of 63 data points available for analysis. For analysis, the following measurements will be taken for each data point:

(1) collector temperature

(2) inlet and outlet temperature of condensing water

(3) mass flow rate

(4) expander speed

(5) generator output

(6) pressure of R-11 (measured at 4 points in cycle

(7) temperature of R-11 (measured at 4 points in cycle).

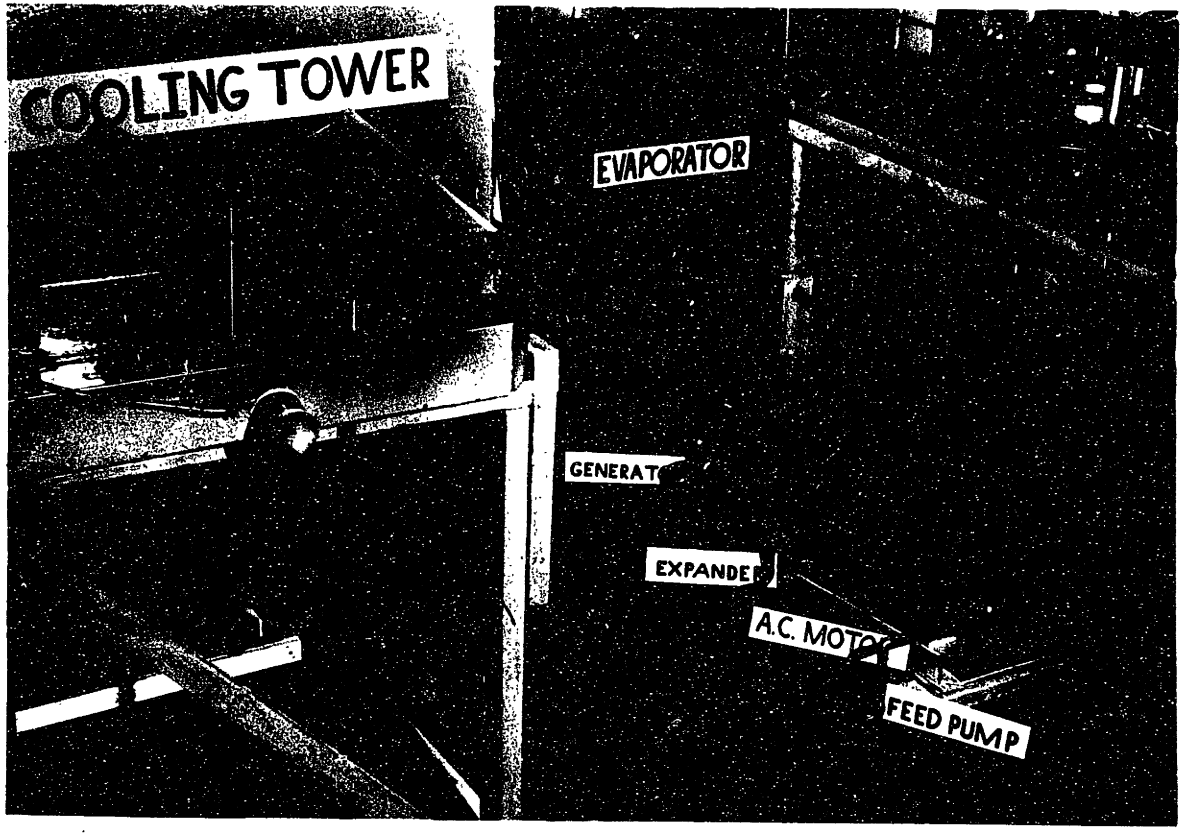

Figure 3 Test Setup of the Experimental Cycle

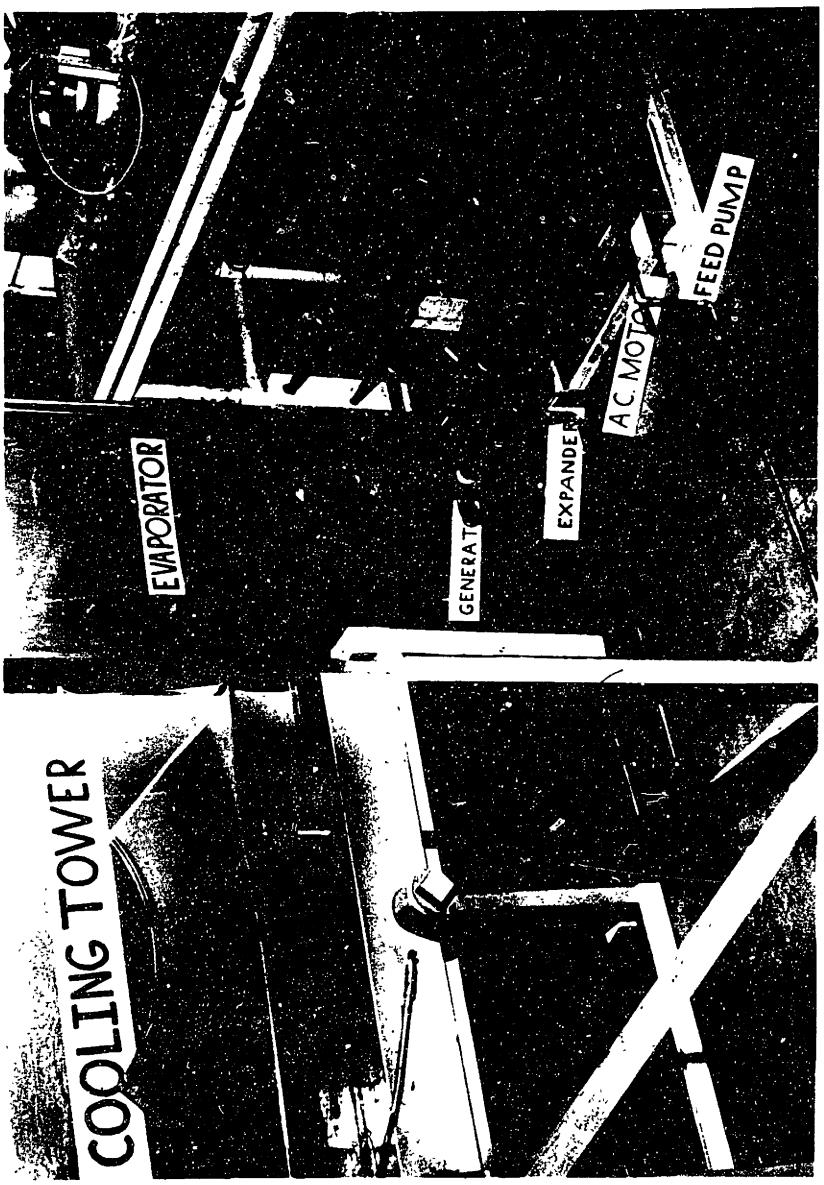

Figure 2 Test Setup of the Experimental Cycle

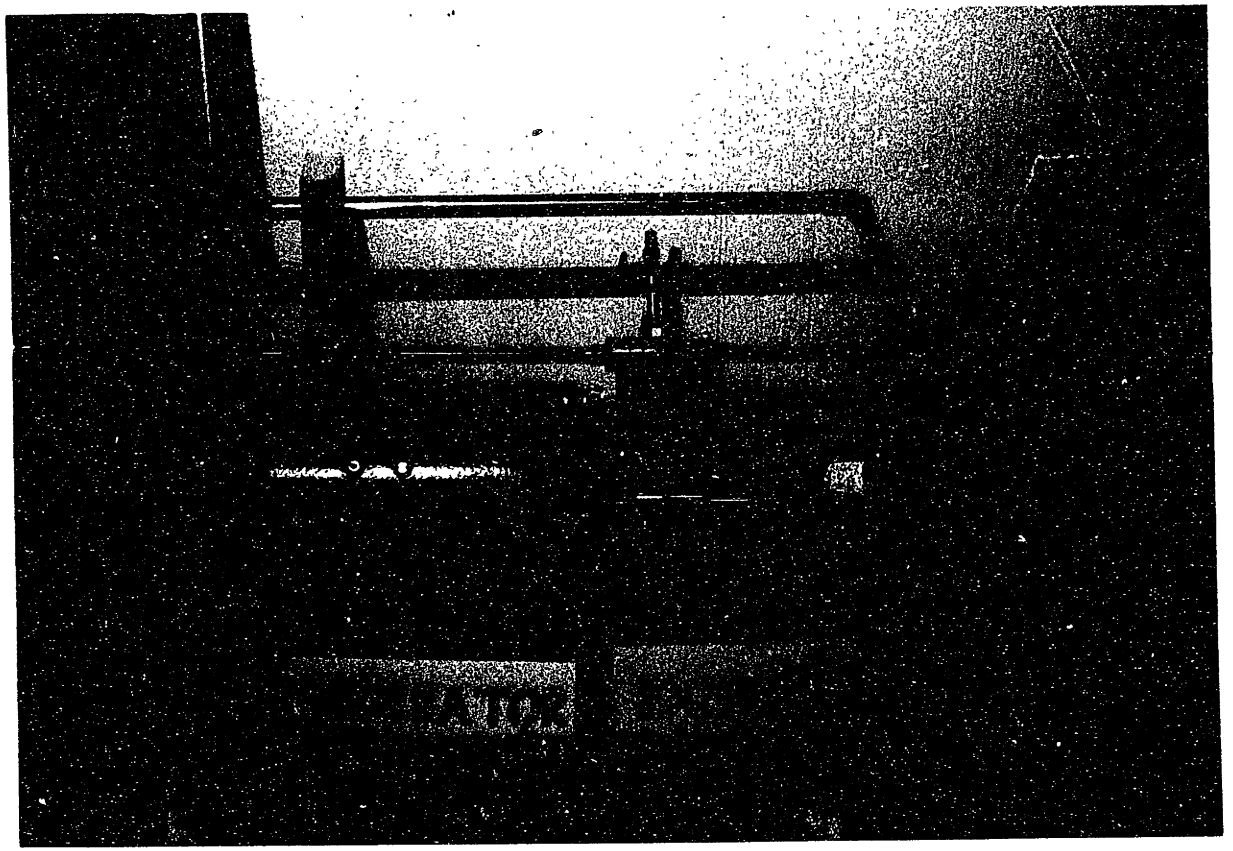

Figure 4 Test Setup of the Expander and Generator

Figure 4 Test Setup of the Expander and Generator

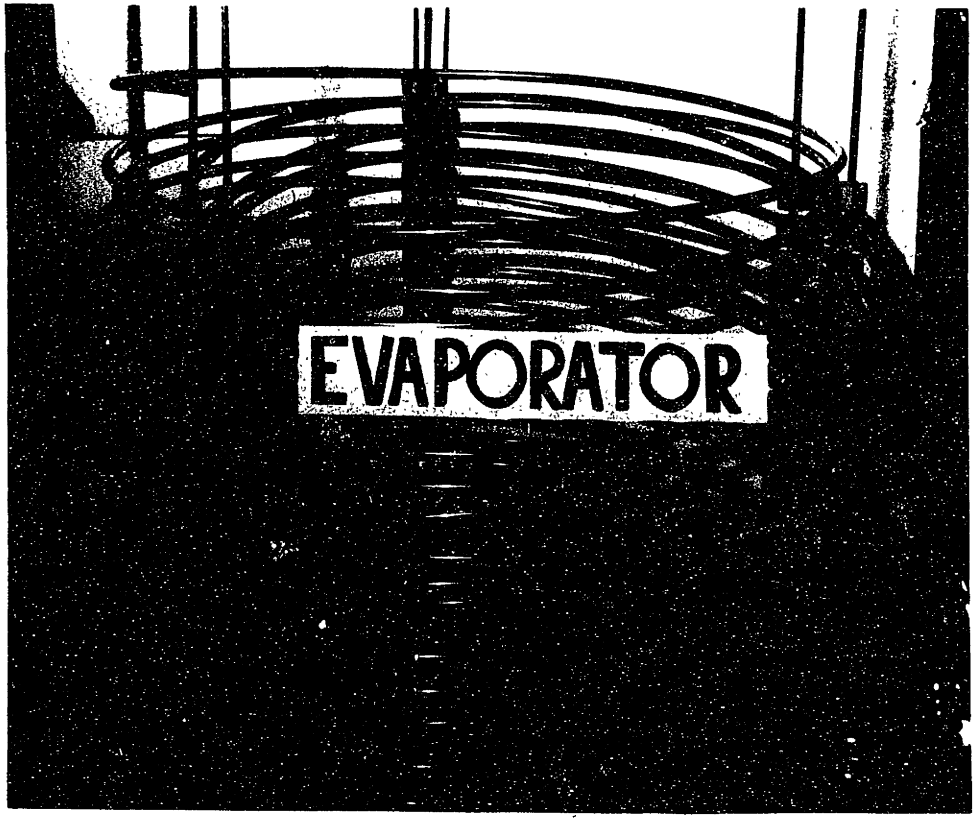

Figure 5 Test Setup of the Evaporator

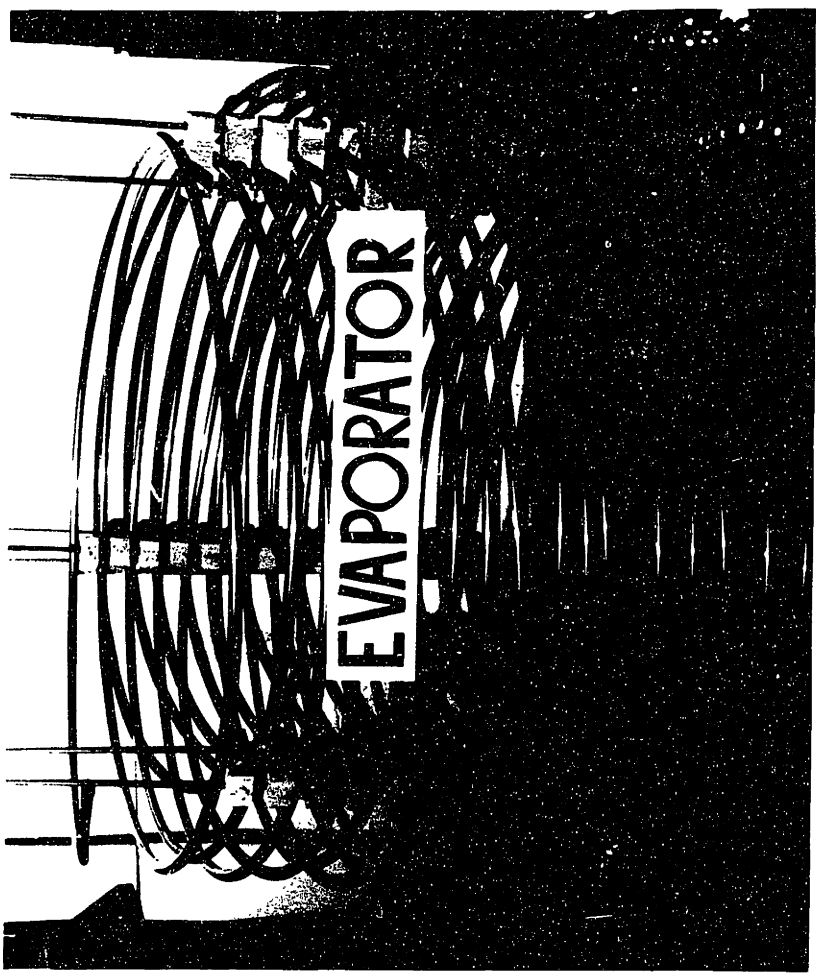

Figure 5 Test Setup of the Evaporator

General Characteristics and Loss Mechanisms of Rotary Vane Expanders

At present, a fair amount of research is being conducted on the use of multi-vane expanders for solar energy applications. The major research effort, undertaken at General Electric under the direction of Spurgeon Eckard, is developing expanders for both steam and high molecular weight working fluids (including R-11). Brake efficiencies as high as 84% for R-11 are reported. The major problem with these expanders has been with friction and corresponding wear, but extrapolated tests have shown that over 20,000 hours of life can be expected for some applications. If improved materials are found, longer lifetimes may be possible.

The rotary-vane expander has several characteristics which make it suitable for solar energy applications in the 1 to 20 Hp range. Some of these characteristics, as cited in the Eckard acticles, are:

(1) easy machining to tight tolerances

(2) conventional shaft seals and anti-friction bearings

(3) easy lubrication

(4) self-compensating for wear

(5) no dynamic valves or gear train

(6) intrinsically balanced

(7) high brake efficiency over a wide range of shaft

power, speed, mass flow, and vapor pressure

(8) High torque at low or zero speed (self starting under load)

(9) speed comparable with driven equipment such as generators

(10) relatively high Volumetric Expansion (10+)

(11) easily adjustable expansion ratio

(12) high tolerance for a wide range of vapor quality (avoids wet vapor erosion and liquid compression damage)

(13) simple control system possible

(14) good life potential.

Discussion of the above characteristics is beyond the scope of this thesis, except as it directly relates to the expander we are testing. The reader is referred to Eckard's articles (4,5) for additional information and references on these characteristics.

Loss Mechanisms

Several mechanisms contribute to the reduction of efficiency in multi-vane expanders. The major loss mechanisms are:

(1) internal leakage

(2) friction

(3) heat transfer to the motor

(4) under or over expansion

and (5) breathing losses.

This section will briefly analyze each loss mechanism, and describe test apparatus used in other studies to measure the contribution of each mechanism.

Internal Leakage

One of the major loss mechanisms in vane expanders is internal leakage; working fluid leaks between the vanes and end plate without exerting pressure on the vanes and performing work. The expander efficiency, examining only leakage losses, is given by Eckard[4] as $\eta_L = 1 - F_1$, where F_1, the leakage fraction of the working fluid, is defined as:

$$F_1 = \frac{\text{(total measured inlet mass flow)} - \text{(theoretical mass flow)}}{\text{(total measured inlet mass flow)}} \quad \text{(eq 1)}.$$

The leakage fraction is thus determined by measuring the system mass flow rate, and calculating the theoretical no-leakage mass flow rate.

In a study by Robertson and Wolgemuth,[10] the effect of end clearance on the leakage fraction is investigated using 150 and 500 psia steam. The study reports that leakage flow rate is approximately proportional to the third power of the end clearance. With 150 psia steam, and an expander speed of 1000 rpm, the study reports a drop in expander brake efficiency of 8% with a .001" clearance, increasing to 55% with a .002" clearance. With 500 psia steam, this drop amounts to 40% with a .001" clearance, and 70% with a .002" clearance. The drop in efficiency, given a constant ex-

pander speed, increases with increasing pressure because the greater pressure force drives more air between the vanes and the end plate. Similiarly, the drop in efficiency, given a constant supply pressure, decreases with increasing speed, because the working fluid has less time to leak from one compartment to another.

Frictional Losses

The power losses due to friction can be estimated by using the relation

$$F_f \sim \mu_e m_v r\, v_r^3 \qquad \text{(eq 2), where}$$

F_f = total frictional loss

m_v = the mass of the vanes

μ_e = the vane/stator coefficient of friction

r = the mean radial position of the vanes

and v_r = the rotor velocity.[4]

Eckard suggests low density vane materials, low speed operation (1200-1800 rpm max.), and selective injection of a liquid lubricant into the expander to minimize frictional losses. Frictional losses in the Robertson-Wolgemuth expander, under operating conditions of 1000 rpm, 150 psia steam inlet, and .05 coefficient of friction, were approximately 10%. For this expander, a liquid lubricant was not used.

The method of experimentally determining frictional losses in vane expanders is fairly complex. In the Robert-

son-Wolgemuth expander, piezoelectric pressure transducers were installed in one end plate of the expander. With the control volume pressure as a function of rotor position known, calculation of the work done by the fluid on the vanes could be performed. The difference between this work and the shaft work as measured by the dynamometer was considered equal to the frictional loss.

Heat Transfer Losses

The third loss mechanism listed, heat transfer to the rotor, can be caused by simple heat transfer from the working fluid to the expander, or by condensation on the expander. The Robertson-Wolgemuth study tried measuring heat loss by mounting a Bendersky surface thermocouple in the expander rotor, with the thermocouple signal taken from the rotor through a mercury slip ring.[10] The output of the thermocouple was used to measure the heat transfer between the steam and the rotor as a function of rotor position, and also determine the amount of steam condensing on the rotor. For their studies, losses due to heat transfer were small when compared to friction and leakage.

Under or Over Expansion Losses

A fourth loss mechanism in multi-vane expanders is under or over expansion of the working fluid. In one study using R-11 as the working fluid, Eckard studied the effect of under and over expansion on the brake efficiency of the

expander. He reports that an increase or decrease of 50% in the ideal pressure ratio for an expander with a volumetric expansion ratio of 3.37 leads to a brake efficiency decrease of approximately 20%. This loss in efficiency is important for solar energy applications because the boiler and condenser temperature will vary with solar insolation and local weather conditions, so the need to maintain a reasonable efficiency over a wide range of operating pressures is desired.

Breathing Losses

Breathing losses occur because some of the working fluid is prematurely expanded in entering the expander. Eckard claims that because the vane expander does not have any dynamic inlet valves, breathing losses can be reduced to insignificant values with proper design.[4]

Analysis of Component and Cycle Efficiency

Estimated efficiency of the 16AM motor

Gast Mfg. Corp. has provided us with information on the torque vs speed characteristics of the 16AM motor using compressed air (figures 7 and 8). Using this data, an analysis of the efficiency of the power cycle as a function of the flow rate of compressed air is given in Appendix 1. As this analysis indicates, the brake efficiency of the vane motor using compressed air is 19.8% at 500 rpm, and 30.2% at 1000 rpm. The leakage fraction is estimated in Appendix 2, and leakage is found to be the major cause for this low efficiency. Leakage fractions of .787 at 500 rpm and .638 at 1000 rpm are calculated, lowering the maximum possible efficiency once leakage losses are included to 21.3% at 500 rpm and 36.2% at 1000 rpm.

In predicting the mass flow rate of R-11 necessary to produce the same outputs, I will assume that the expander's overall efficiency at a given rpm using R-11 is the same as the overall efficiency using compressed air. Based on this analysis, presented in Appendix 3, 29.0 lbs/min of R-11 are needed to produce 1.04 kw at 500 rpm, and 34.1 lbs/min are needed to produce 1.69 kw at 1000 rpm.

Feed pump efficiency

The feed pump chosen will be driven by a ½ Hp (.373 kw) motor running at 1725 rpm. It will be used to pump 3.13

gpm of R-11 from 16.2 to 79.4 psia. The equation for the power consumption of an ideal pump working with 100% efficiency is[6]

$$W_{ip} = v\,(P_{in} - P_{out}) \qquad \text{(eq 3)}$$

where v is the volume of the liquid (ft^3/lbm)
and P is the pressure (lbf/ft^2)

Relating this to our process,

$$v_{(R\text{-}11,\ 80\ F)} = .011\ ft^3/lbm$$

$$\text{so } W_{ip} = (.011\ ft^3/lbm)(79.6\text{-}16.2\ lbs/in^2)(144\ in^2/ft^2)$$

$$= 98.9\ ft\text{-}lbs/lbm$$

For operation at 500 rpm, 29 lbs/min (2.36 gal/min) of R-11 must be pumped, so a perfectly matched and 100% efficient motor-pump would require

$$(98.9)(29) = \frac{2868\ ft\text{-}lbs/min}{44270\ ft\text{-}lbs/min/kw} = .0648\ kw$$

At 1000 rpm, 34.1 lbs/min must be pumped, corresponding to a power comsumption of (98.9)(34.1)/44270 = .0762 kw. At 500 rpm, the motor-pump efficiency is .0648 kw/.373 kw = 17.4%. Similiarly, at 1000 rpm the motor-pump efficiency is .0762/.373 = 20.4%

The above analysis assumes that the pump can actually pump 3.13 gpm of R-11 to 79.4 psia with a ½ Hp motor. From manufacturers information, .40 Hp is needed to pump this volume of water to 80 psia. The density of R-11 is approximately 1.5 times the density of H_2O, however, so the pump-

ing power will be higher. Without testing, the additional power needed by this pump to pump the R-11 to 80 psi cannot be determined.

Cycle Analysis for 2 mass flow rates of R-11

To give a clearer picture of the energy and mass flow rates, expected temperatures and pressures, and overall efficiency of the power cycle, an analysis of the state and performance of the cycle will be conducted under the following conditions:

(1) boiler water temperature = 210°F

(2) condenser water temperature = 60°F (Inlet temp. = 50°F, outlet temp. = 70°F)

(3) mass flow rates of R-11 (A) G = 30 lbm/min

(B) G = 35 lbm/min

As outlined in the experimental program, the following measurements will be taken for analysis.

(1) collector temperature

(2) inlet and outlet temp. of condensing water

(3) R-11 mass flow rate (G)

(4) expander speed

(5) generator output

(6) R-11 pressure (at 4 points in cycle)

(7) R-11 temperature (at 4 points in cycle)

Prediction of the above measurements for 30 lbm/min and 35 lbm/min mass flow rates is performed in Appendix 6. The

results of this analysis are presented in Table 1. The location of the temperature-pressure points referred to are illustrated in Figure 6.

In making this analysis, the pressure drops due to viscous losses and changes in working fluid velocity are assumed small. Analysis of these losses is appropriate for a complete analysis, but is not performed for this thesis.

Overall analysis of the experimental cycle's efficiency

Only a small percentage of the sun's energy used to heat a low temperature solar collector is transformed into electricity. This percentage is very low, first because of limitations imposed by the second law of thermocynamics, and second because of inefficiencies in the actual apparatus. In this section, the experimental cycle is analysed first in terms of its potential efficiency. An analysis of the actual cycle efficiency once losses in the cycle components are accounted for is then conducted.

The highest theoretical efficiency of our power cycle, the Carnot efficiency, is equal to

$$= \frac{T_H - T_L}{T_H} \quad [6] \qquad \text{(eq 4)}$$

with T_H and T_L in °R or °K.

For our cycle:

$$T_H = 210°F = 670°R$$
$$T_L = 60°F = 520°R$$

G (lbm/min)	evaporator T (°F)	condenser T (average) (°F)	expander speed (rpm)	generator output (kw)	bypass valve flow (lbm/min)
30	210	60	500	1.04	8.5

point in cycle	T (°F)	P (psia)	h (Btu/lbm)	(G)(h) (Btu/hr)	(G)(h) (kw)
1	178.3	77.7	112.73	153,900	45.1 → Q_e
2	158.6	59.3	110.60	-3,824	-6.12 → expander output + friction loss
3	89.6	19.4	26.52	-151,350	-44.3 → Q_c
4	92.3	80	27.23	1,270	.37 → feed pump power

G (lbm/min)	evaporator T (°F)	condenser T (average) (°F)	expander speed (rpm)	generator output (kw)	bypass valve flow (lbm/min)
35	210	60	1000	1.69	3.5

point in cycle	T (F)	P (psia)	h (Btu/lbm)	(G)(h) (Btu/hr)	(G)(h) (kw)
1	173.6	72.9	112.23	177,130	51.9
2	143.6	47.6	108.94	-6,909	-2.02
3	93.2	32.9	27.28	-171,486	-50.2
4	95.5	80	27.88	1,270	.37

Table 1 - Cycle Analysis with 30 and 35 lbm/min Flow Rates

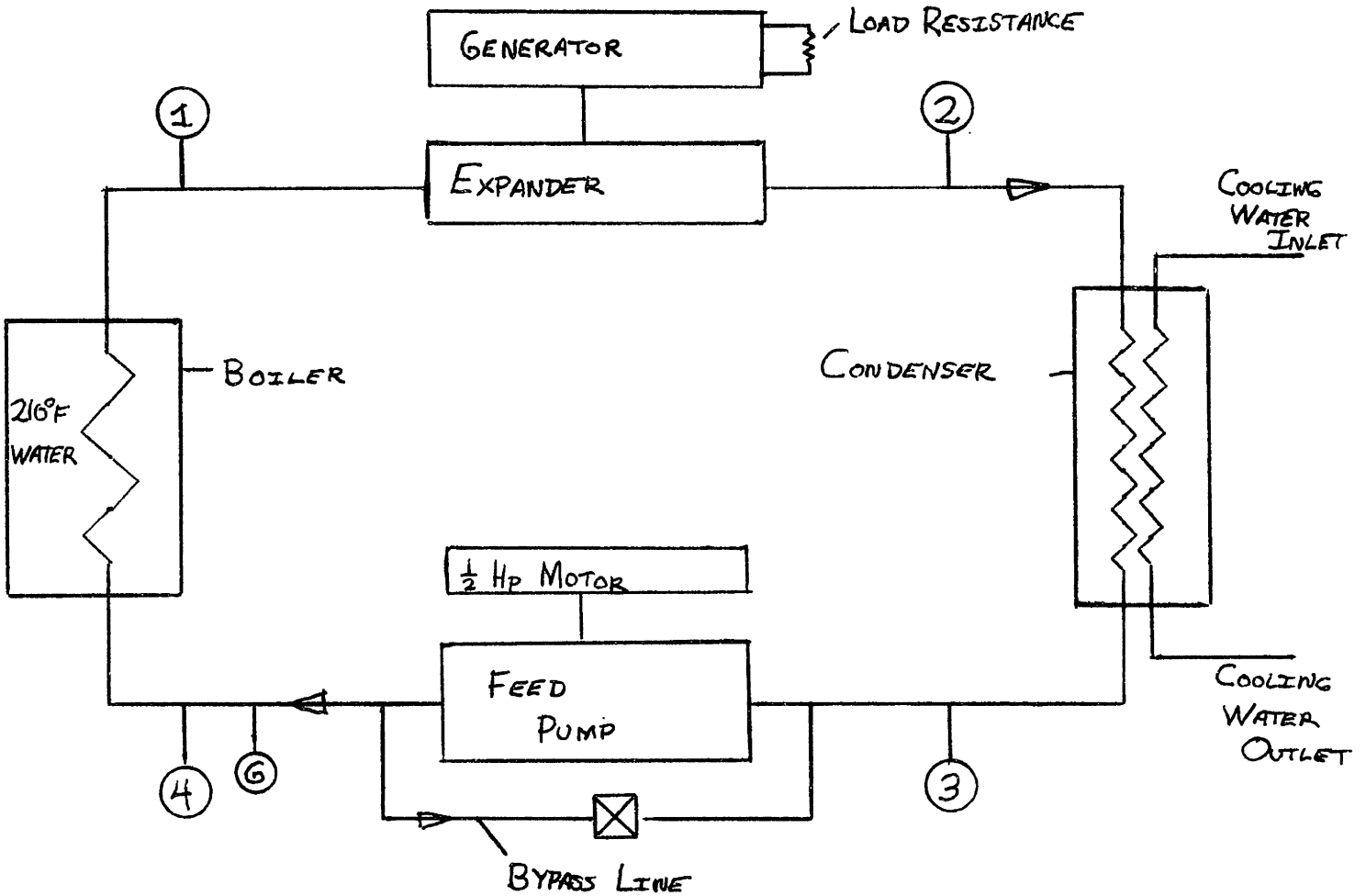

FIGURE 6 - LOCATION OF TEMPERATURE - PRESSORE MEASUREMENT POINTS IN THE EXPERIMENTAL CYCLE

$$= \frac{670 - 520}{670} = 22.4\%.$$

Due to the temperature drops across the evaporator and condenser, the temperature range experienced by the working fluid is less than the range initially used to calculate the Carnot efficiency. For the cycle at 500 rpm,

$$T_{(v,1)} = 178.3^{\circ}F$$

and $$T_{(l,3)} = 89.6^{\circ}F$$

The Carnot efficiency corresponding to this temperature differential is

$$= \frac{638 - 550}{638} = 13.8\%$$

As working fluids are not thermodynamically perfect, the cycle efficiency is further reduced by the enthalpy change of the working fluid over the above temperature differential. This efficiency, referred to as the Rankine efficiency, is

$$\eta_R = \frac{h_{(v,178.3)} - h_{(v,89.6)}}{h_{(v,178.3)} - h_{(l,89.6)}} = \frac{(112.73 - 102.72)}{(112.73 - 26.52)} = 11.6\% \text{ or } .84\,\eta_c$$

Our expander has an efficiency, $E_e = 19.8\%$ of Rankine as calculated in Appendix 1. The overall conversion efficiency from heat input to mechanical power output is therefore $\eta_T = (E_e)(\eta_R) = (.198)(.116) = 2.30\%$. If the power imput to the feed pump is included, the cycle efficiency be-

comes

$$\eta\,(T + fp) = \frac{W_e - W_{pump}}{W_e}\eta_T = \frac{1.04 - .373}{1.04}\eta_T = 1.46\%$$

Similiarly, for the cycle at 1000 rpm

$$\eta_R = \frac{h_{(v,173.6)} - h_{(v,93.2)}}{h_{(v,173.6)} - h_{(l,93.2)}} = \frac{112.23 - 103.14}{112.23 - 27.28} = 10.7\%$$

The expander has an overall efficiency E_e = 30.2% of Rankine at 1000 rpm, making the heat input to mechanical output efficiency $\eta_T = (E_e)(\eta_R) = (.302)(.107) = 3.23\%$. With power from the feed pump included,

$$(T + fp) = \frac{1.69 - .373}{1.69}\eta_T = 2.52\%$$

The above analysis illustrates that the components used for our test cycle are not very efficient. The evaporators and condensers cut the efficiency of the cycle by about 40%, and the expander cut the efficiency by approximately 80% at 500 rpm and 70% at 1000 rpm. For solar energy applications the collector costs are generally much higher than the power cycle cost. The design of an efficient power cycle is therefore very important to keep collector costs at a minimum.

Conclusion

Research on our experimental power cycle can continue in several areas. First, the current cycle should be tested, both to see what problems will arise in actual experimentation, and to compare experimental results with those predicted in this thesis.

To improve cycle efficiency, a partial solution is to increase the size of the evaporator's heat exchange area. Another possibility is to modify the air motor along the lines suggested by Eckard. Such modifications will make the air motor more efficient, and also, because of lowered heat input, reduce the evaporator and condenser temperature differentials, further increasing efficiency.

To vary the expander output to match load requirements at different times of the day, and also to shut off the expander if collector temperature becomes too low to make power production efficient, an electrical-mechanical control system for the power cycle must be designed and tested.

To predict cycle performance for a large variety of collector temperatures, condensing temperatures, and R-11 mass flow rates, a computer program to perform the cycle analysis, following the procedure used in Appendix 6, would be appropriate.

Appendix 1 - Estimated Expander Efficiency

One method of calculating the efficiency of the expander is to compare the work ideally available in a given volume of air undergoing expansion from 80 psia to 16.7 psia to the shaft output of the air motor. By this method, the efficiency of the expander $E_e = \frac{W_e}{\Delta H_{air}}$, where

W_e is the shaft power of the expander

and ΔH_{air} is the enthalpy change of the compressed air.

For quasi-static and adiabatic expansion, the volumetric expansion can be calculated from the relation[3] $P_1V_1^{\gamma} = P_2V_2^{\gamma}$, or $\frac{1}{\gamma}(\ln P_1/P_2) = \ln(V_2/V_1)$. For the process being investigated,

$P_1 = 80$ psia $\qquad T_1 = 529^{\circ}R$ $(294.25^{\circ}K)$

$P_2 = 16.7$ psia

and $\gamma = 1.4$.

Substituting, and solving for V_2/V_1, we find that $1.12 = \ln(V_2/V_1)$, or $V_2/V_1 = 3.06$. Similiarly, the final temperature T_2 can be calculated from the relation[3] $T_1V_1^{\gamma-1} = T_2V_2^{\gamma-1}$. Substituting values for T_1, γ, and V_2/V_1, $T_2 = 338.2^{\circ}R$. $(188^{\circ}K)$.

For the air motor operating at 500 rpm, the Gast Mfg. Corp. gives the volume flow rate of free air as 85 ft^3/min (see Figure 8). Assuming that the state of this free air is $529^{\circ}R$., and 16.7 psia, the mass flow rate can be determined from the ideal gas law, PV=mRT (m=PV/RT). Substituting,

$$m = \frac{(2405\ lbf/ft^2)(85\ ft^3/min)}{(53.34\ ft{\cdot}lbf/lbm{\cdot}^\circ R)(529^\circ R)} = 7.24\ lbm/min.$$

Knowing the mass flow rate, ΔH_{air} can now be calculated. From Thermodynamic Properties of Refrigerants[12] (p. 313):

H_{air} (80 psia, 294.25°K) = 12,197 Joules/mole

H_{air} (16.7 psia, 188°K) = 9,118 Joules/mole

ΔH_{air} = 12,197 - 9,118 = 3,079 Joules/mole

Using the conversion factors

1 joule = .001 kw·sec
1 lbm = 453.6 grams
and 1 mole air = 28.97 grams

a mass flow rate of 7.24 lbm/min corresponds to an enthalpy change of the air

$$\Delta H_{air} = 7.24\ \frac{lbm}{min}\ \frac{453.6\ g}{lbm}\ \frac{1\ mole}{28.97\ g}\ \frac{3079\ J}{mole}\ \frac{.001\ kw{\cdot}sec}{1\ J}\ \frac{1\ min}{60\ sec} =$$

5.81 kw.

The actual output of the air motor at this speed, using (torque vs velocity) data supplied by the Gast Mfg. Corp. (Figure 7), is W_e = (Torque)(Velocity) = (195 in-lbs)(1 ft/12 in)(52.34 rad/sec) = 851 ft-lbs/sec = 1.15 kw.

By the above analysis, the brake efficiency of the air motor at 500 rpm is $E_e = \frac{W_e}{\Delta H_{air}}$ = (1.15)/(5.81)=19.8%. Using the same analysis at 1000 rpm, the expander efficiency E_e = 2.06/6.83 = 30.2%.

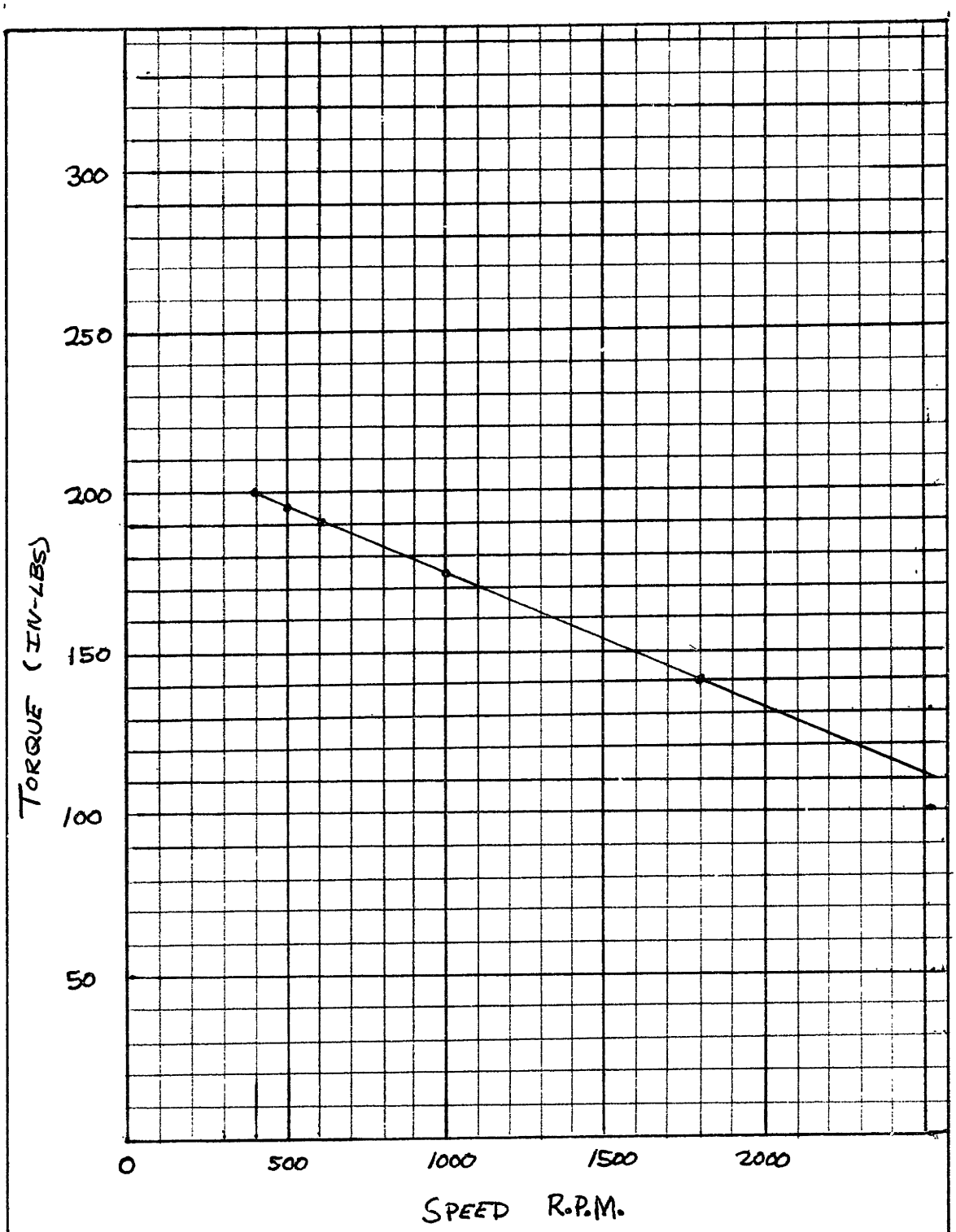

FIGURE 7- TORQUE VS. SPEED PLOT OF THE TEST EXPANDER (COURTESY OF GAST MFG. CORP.)

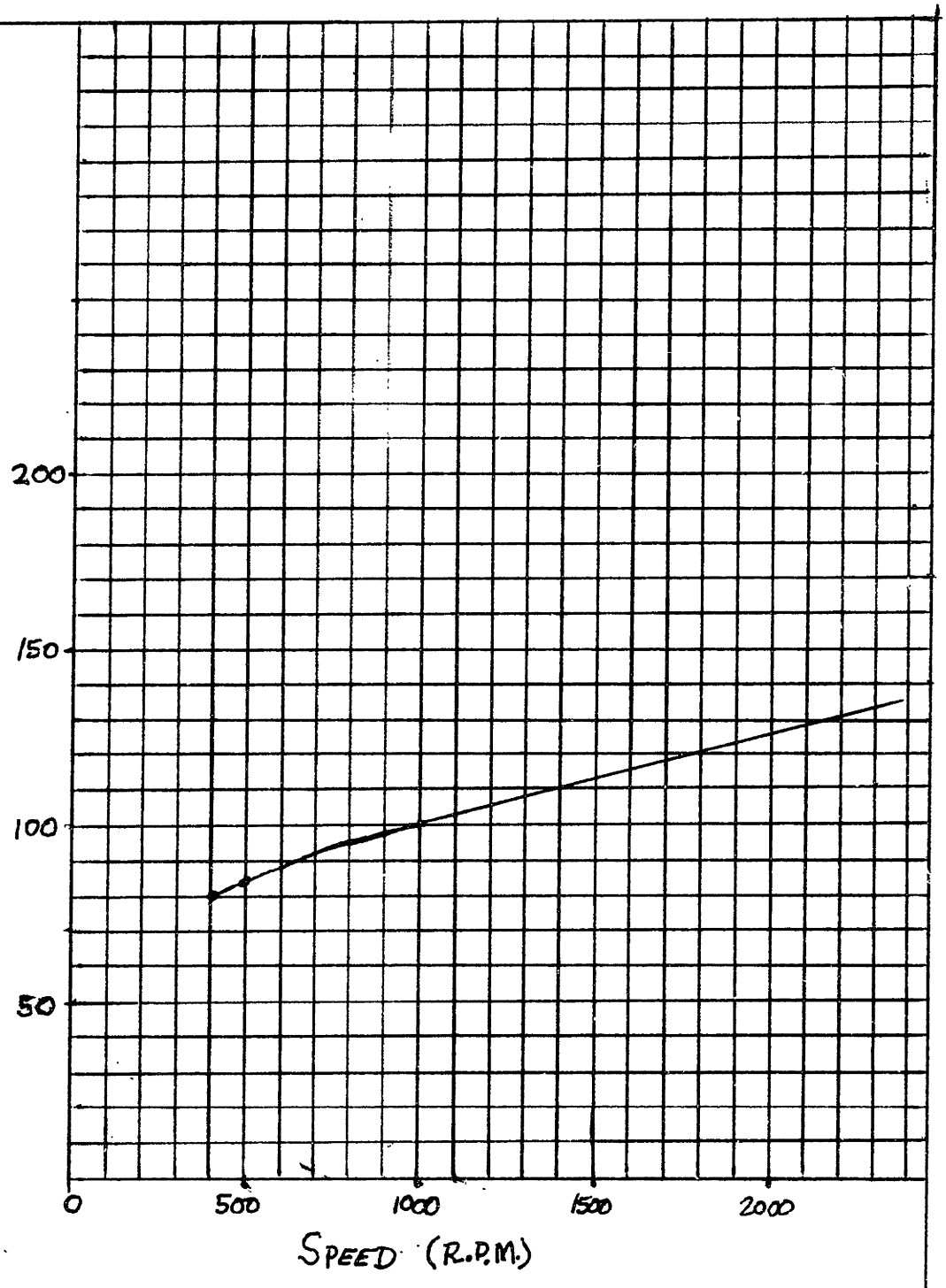

FIGURE 8- AIR FLOW RATE VS. SPEED PLOT OF THE TEST EXPANDER

(COURTESY OF GAST MFG. CORP.)

Appendix 2 - Estimated Leakage Fraction of Compressed Air in Expander

As calculated in Appendix 1, the estimated mass flow rate of air with the expander running at 500 rpm is 7.24 lbs/min. The loss of efficiency due to leakage can be calculated by use of the equations

$\eta_L = 1 - F_1$, where $F_1 = \dfrac{(\text{total measured inlet mass flow}) - (\text{theoretical mass flow})}{\text{total measured mass flow}}$,

as described in the main text (eq 1).

The theortical mass flow rate can be determined by calculating the no-leakage volume flow rate of air in the initial compartment of the expander, and using the ideal gas law (PV=mRT) to calculate the no-leakage mass flow rate.

As Figure 2 illustrates, the cross sectional area of the initial volume of air is .28 in^2. Multiplied by the width of the expander (4.5 in), and added to the volume of air in the rotor used for the inlet of air (.91 in^3), the initial control volume for the expander is (.28 in^2)(4.5 in) + (.91 in^3) = 2.17 in^3. At 500 rpm, air will be allowed to flow into a compartment of this size (500 rpm)(600 compartments/rpm) = 3000 times/minute, giving a no-leakage volume flow rate of

$$(3000/\text{min})(2.17\ in^3) = \frac{(6580\ in^3/\text{min})}{(1728\ in^3/ft^3)} = (3.76\ ft^3/\text{min}).$$

The mass flow rate corresponding to this is m=PV/RT, or

$$m = \frac{(11520\ \text{lbs/ft}^2)(3.75\ \text{ft}^3/\text{min})}{(53.34\ \text{ft}\cdot\text{lbs/lbm}^\circ\text{R})(529^\circ\text{R})} = 1.54\ \text{lbs/min.}$$

$$F_1 = \frac{7.24 - 1.54}{7.24} = .787$$

$$\eta_L = 1 - F_1 = 21.3\%$$

By this analysis, the maximum brake efficiency of the expander, if one looks only at losses due to leakage, is 21.3%. For the expander operating at 1000 rpm, a corresponding analysis yields a leakage fraction $F_1 = .638$ and $\eta_L = 1 - F_L = .362$.

Appendix 3 - Estimated Mass Flow Rates of R-11 at 500 and 1000 rpm

The R-11 for this test cycle is designed to be heated to a temperature of 180°F, and to be condensed at a temp. of 80°F. Enthalpy values for R-11 at these temperatures are given in Figure 9 below.

$h_{(v,180^\circ F)}$= 112.909 Btu/lbm (density=1.8 lbs/ft^3)

$h_{(l,180^\circ F)}$= 45.774 Btu/lbm (density=83 lbs/ft^3)

$h_{(v,\ 80^\circ F)}$= 101.583 Btu/lbm (density=.402 lbs/ft^3)

$h_{(l,\ 80^\circ F)}$= 24.523 Btu/lbm (density=92 lbs/ft^3)

Figure 9 - Enthalpy and density values for R-11 at 80 and 180°F

From Figure 9, $W_{net} = h_{(v,180^\circ F)} - h_{(v,80^\circ F)} = 11.4$ Btu/lbm. To achieve 1.15 kw using R-11, and assuming 100% expander efficiency, a mass flow rate of

$$G = \frac{(56.9 \text{ Btu's/kw-min})(1.15 \text{ kw})}{(11.4 \text{ Btu's/lbm})} = 5.74 \text{ lbm/min}$$

is necessary.

Assuming 19.8% efficiency, the necessary mass flow rate of R-11 is G = (1/.198)(5.74) = 29.0 lbs/min.

Similiarly, at 1000 rpm (1/.302)(10.3) = 34.1 lbs/min is necessary to achieve the 2.06 kw output.

Appendix 4 - Temperature Differential Across the Evaporator

The temperature differential across the evaporator can be calculated from the equation

$$T_e = Q/AU \qquad \text{(eq A4.1)}$$

(Heat, Mass, and Momentum Transfer, p. 100), where

Q= the heat transferred across the evaporator

A= the area of the copper tubes

and U= the overall heat transfer coefficient.

$$U = \frac{1}{\frac{1}{h_i} + \frac{x_a}{K_a} + \frac{1}{h_o}} \qquad \text{(eq A4.2), where}$$

h_i= the contact coefficient of heat transfer between the evaporating R-11 and the copper tubing

h_o= the contact coefficient of heat transfer between the copper tubes and the outside water

x_a= the thickness of the copper tubing

and K_a= the heat transfer coefficient of the copper tubing

Calculation of the heat transfer coefficient h_i, x_a/K_a, and h_o with the corresponding calculation of U, is given below.

(A) Value of h_i

As listed in Refrigeration, Air Conditioning, and Cold Storage, p. 806-807, the value of h_i between evaporating R-11 and the copper tube is approximately 2000 Btu's/ft^2-hr^oF.

(B) Value of K_a/x_a

$x_a = 1/16" = 0.00521$ ft

$K_a = 220$ Btu/ft-hr-°F for copper[11]

so $K_a/x_a = \frac{200 \text{ Btu/ft-hr-°F}}{0.00521 \text{ ft}} = 42{,}200 \text{ Btu/ft}^2\text{-hr-°F}$

(C) Value of h_o

H_o is the value of the heat transfer coefficient between the copper tube and the water due to natural convection. As the values of the other two transfer coefficients are relatively large, the value of h_o will have the greatest effect on the heat transfer between the water and the R-11. From Heat, Mass, and Momentum Transfer (p. 159), for free convection and laminar flow:

$h_o = (Nu)K/y_o$ (eq A4.3), where

$Nu = \frac{(0.676)Pr^{\frac{1}{2}}}{(.861 + Pr)}(Gr_x/4)^{\frac{1}{4}}$ (eq A4.4)

$Gr_x = \frac{g_x y_o^3 (T_w - T_c)}{\nu^2}$ (eq A4.5)

$y_o = \pi D/2$ (correction factor for a tube)

$K = .394$ Btu/hr-ft-°F

and, for water at 200°F

$\beta = 0.4 \times 10^{-3}/\text{R}$

$\nu = 0.012$ ft^2/hr

$Pr = 1.9$

Substituting the above values in equation A4.5 and A4.4, we

obtain Gr= 6.5 x 10^6, GrPr = 1.24 x 10^7, indicating that flow is laminar, and Nu= 34.4. Using D= 0.0417,

$$h_o = \frac{(34.4)(.0394 \text{ Btu/hr-ft- F})}{0.0654 \text{ ft}} = 207 \text{ Btu's/ft-hr-}^\circ\text{F.}$$

(D) Calculation of U

$$U = \frac{1}{\frac{1}{2000} + \frac{1}{42200} + \frac{1}{207}} = 187 \text{ Btu/ft}^2\text{-hr- F}$$

(E) Calculation of T_e

T_e= Q/QU= Q/4900 (eq A4.6), where

A= (200 ft)(/24 ft^2/ft)= 26.2 ft^2

U= 187 Btu/ft^2-hr-$^\circ$F,

Q is in Btu/hr, and T is in $^\circ$F.

Appendix 5 - Temperature Differential Across the Condenser.

The temperature differential across the condenser can be calculated by use of equations A4.1 and A4.2, where, for the condenser,

h_i = the contact coefficient of heat transfer between the condensing R-11 and the radiator

h_o = the contact coefficient between the cooling tower, water and the radiator

and all other variables have the same definitions as before.

Calculation of the heat transfer coefficients h_i, x_a/k_a, and h_o, with the corresponding calculation of U, is given below.

(A) Value of h_i

Approximate heat transfer coefficients are available for organic liquids as a function of the vapor mass flow rate per cross sectional area of the flow path (G_m= lbm/hr-ft^2). As given in the truck radiator description (page 17), the cross sectional area of the flow path for the condenser is .156 ft^2. The vapor mass flow rate for our experiments will be 29.0 lbm/min (1740 lbm/hour) at 500 rpm,

and 34.1 lbm/min (2046 lbm/hour) at 1000 rpm.

The values of G_m for the above mass flow rates are:

at 500 rpm, $G_m = (1740 \text{ lbm/hr})(.156 \text{ ft}^2) = \frac{9280 \text{ lbm}}{\text{hr-ft}^2}$,

at 1000 rpm, $G_m = (2046 \text{ lbm/hr})(.156 \text{ ft}^2) = \frac{13,094 \text{ lbm}}{\text{hr-ft}^2}$.

Using data from Figure 13.2 of Heat Exchanger Design[7] for $G_m = 9280$, $h_i \approx 250$, and for $G_m = 13{,}094$, $h_i \approx 325$. To be conservative, I will use the lower value for h_i, 250 Btu/hr-ft^2-°F.

(B) Value of x_a/K_a

Two values of heat transfer through the copper need to be determined; one value for heat transfer through the rectangular copper tubes, and another value for heat transfer through the fins.

(1) Heat transfer through the copper tubes

$x_a = 1/32" = .00260$ ft

$K_a = 220$ Btu/ft-hr-°F for copper[11]

$x_a/K_a = .00260/220 = .00001184$ ft^2-hr-°F/Btu

$K_a/x_a = 84{,}400$ Btu/ft^2-hr-°F

(2) Heat transfer through the fins

Because the rectangular tubes are spaced approximately .75" apart, heat transferred to the fins will travel an average distance of .75"/4 = .1875" before it is transferred to the cooling water. The heat transfer coefficient for the fins is therefore $K_a/x_a = 220/.0156 = 14{,}080$ Btu/ft^2-hr-°F, where ft^2 for this equation is the net surface area of the fins through which heat flows outward from the tubes. For a given tube-fin joint, this area is equal to the thickness of the fin (.005") times the contact length with the tube (2.375 in), or 8.25×10^{-5} ft^2. The number of tube-fin

joints in the radiator is (180 tubes)(9 fins/inch)(30 in) = 48,600 joints, so the net surface area for all tube-fin joints = $8.25 \times 10^{-5} \times 48{,}600 = 4.01$ ft^2.

In calculating U in equation A4.2, the surface areas over which h_i, h_o, and x_a/K_a act are assumed to be equal to A. It this is not the case, these values must be adjusted to give the correct heat transfer when A is used in that equation. Letting A= 75 ft^2, I will define $(K_a/x_a)^* = (K_a/x_a)(A_{fins}/A) = (14{,}080)(4.01/75) = 753$ Btu/ft^2-hr- F. Since the surface area of the rectangular tubes is 75 ft^2, a substantial amount of heat will be transferred directly from the tubes to the cooling water, without being transferred to the fins. The approximate percentage of the heat not being transferred to the fins is $(A_{tubes})/((A_{tubes}) + (A_{fins})) = 75/285 = 26.3\%$. The value of (K_a/x_a) to be used in the calculation of U, which I shall define as $(K_a/x_a)^{**}$, is therefore:

$$(K_a/x_a)^{**} = \frac{1}{\frac{.263}{84{,}400} + \frac{.737}{753}} = 1019 \ \frac{\text{Btu}}{\text{hr-ft}^2\text{- F}}.$$

(C) Value of h_o

Assuming natural convection, the same equations as used in Appendix 4 can be used to calculate h_o, the contact coefficient between the cooling water and the radiator. For this case;

y_o= .11 in= the distance between fins

$k = 0.394$ Btu/hr-ft-^{o}F

$g = 32.2$ ft/sec^2 $= 4.17 \times 10^8$ ft/hr^2

and, for water at 60 F,

$\beta = .08 \times 10^{-3}$/ R

$\nu = .044$ ft^2/hr

and $P_r = 7.9$.

Substituting these values into equations A4.4, A4.5., and A4.6:

$$G_r = \frac{(4.17 \times 10^8)(.08 \times 10^{-3})(20)(7.7 \times 10^{-7})}{(.044)^2} = 264$$

$$Nu = \frac{(.676)(7.9)^{\frac{1}{2}}}{(.676 + 7.9)}(264/4)^{\frac{1}{4}} = .617$$

$$h_o = \frac{(.617)(.394 \text{ Btu/hr-ft}^2\text{-}^{o}\text{F})}{} = 27.0 \frac{\text{Btu}}{\text{hr-ft}^2\text{-}^{o}\text{F}}$$

As this value of h_o acts over an area of 285 ft^2, $h_o^* = (285 \text{ ft}^2/75 \text{ ft}^2)(h_o) = 102.6$ Btu/hr-ft^2-^{o}F.

(D) Calculation of U

$$U = \frac{1}{\frac{1}{250} + \frac{1}{1019} + \frac{1}{103}} = 68 \text{ Btu/ft-hr-}^{o}\text{F}$$

(E) Calculation of T_c

$T_c = Q/AU = Q/(75)(68) = Q/5100$ (eq A5.1),

where Q is in Btu/hr and T_c is in ^{o}F.

Appendix 6 - Prediction of Cycle Performance

Given the boiler temperature, condensing water temperature, and mass flow rate of R-11, the procedure used for predicting cycle performance is as follows:

(A) Predict the temperature drop across the evaporator and condenser, using an iterative procedure. The procedure also estimates the heat input to the boiler. With the temperature drop known, the temperature at points (1) and (3) in Figure 6 can be calculated from the equations:

$$T_{(R\text{-}11,1)} = T_{boiler} - T_e \qquad \text{(eq A6.1)}$$

and $$T_{(R\text{-}11,3)} = T_{(cooling\ water)} + T_c \qquad \text{(eq A6.2)}$$

(B) The corresponding enthalpy and pressure of R-11 at points (1) and (3) can be found or interpolated from standard tables of saturated liquid and vapor for R-11, as found in Thermodynamic Properties of Refrigerants.[12]

(C) Prediction of the enthalpy at point 2 - The change in enthalpy from point (1) to point (2) is equal to the work performed by the working fluid on the expander (equal to the expander efficiency after leakage (η_L)), minus any heat transfer between the two points. Neglecting heat transfer, $\Delta h_{(v,1-2)} = (h_{(v,1)} - h_{(v,3)})(\eta_L)$, or

$$h_{(v,2)} = h_{(v,1)} - \eta_L(h_{(v,1)} - h_{(v,3)}). \qquad \text{(eq A6.3)}$$

Once the enthalpy at point two is determined, temperature and pressure can again be obtained from tables.

(D) Prediction of the expander output - The expander

output (W_e) can be predicted by multiplying the estimated expander efficiency (E_e), as determined in Appendix 1, by the enthalpy change in the vapor in going from T_1 to T_3; or

$$W_e = E_e(h_{(v,1)} - h_{(v,3)}) \qquad \text{(eq A6.4)}.$$

(e) the pressure at point 4 is estimated as approximately 80 psi, based on data provided by the manufacturer. Testing will determine the exact pressure produced.

(F) The enthalpy change from point 3 to 4, as given in Faire's Thermodynamics[6] for an incompressible fluid, is $h_2 - h_1 = \int_{T_1}^{T_2} c_v dT + v(P_2 - P_1)$. This is simply equal to the energy input from the pump to the fluid, or approximately .373 kw. Rearranging the above equation $\int_{T_1}^{T_2} c_v dT = (h_2 - h_1) - v(P_2 - P_1)$, or $c_v T = .373 - v(P_2 - P_1)$.

From this $T_4 - T_3 = \dfrac{.373 - v(P_2 - P_1)}{c_v}$

The predicted system performance for $T_{boiler} = 210^\circ F.$, $T_{cooling\ water} = 60^\circ F.$, and $G = 30$ lbm/min, using the preceeding procedure, is:

(A) for the evaporator

$$T_e = Q_e/(26.1)(187) = Q_e/4900 \qquad \text{(eq A4.6)}$$

and for the condenser $T_c = Q_c/(75)(68) = Q_c/5100$ (eq A5.1)

Assuming a T_e of $30^\circ F.$ and a T_c of $20^\circ F.$,

the energy flow into the evaporator = $Q_e =$

$$(G)(h_{(v,180^\circ F.)} - h_{(1,180^\circ F)}) =$$

$(1800)(112.909 - 24.523) = 159{,}084$ Btu/hr

To a first approximation,

$T_e = 159{,}084/4884 = 32.6^\circ F.$

$T_c = (159{,}084 - 3900)/5100 = 30.4^\circ F.$ where $3900 = W_e$

$T_{(v,1)} = 210 - 32.6 = 177.4^\circ F.$

$T_{(l,2)} = 60 + 30.4 = 90.4^\circ F.$

To a second approximation

$Q_e = (G)(h_{(v,177.4^\circ F)} - h_{(l,90.4^\circ F)}) = (1800)(112.633 - 26.693) = (1800)(85.93) = 154{,}700$ Btu/hr

so $T_e = 154{,}700/4884 = 31.7^\circ F.$

$T_c = (154{,}700 - 3900)/5100 = 39.6^\circ F.$

Using these values,

$T_{(R-11,1)} = 210 - 31.7 = 178.3^\circ F.$

$T_{(R-11,3)} = 60 + 29.6 = 89.6^\circ F.$

(B) From tables,

$P_{(v,1)} = 77.7$ psia

$h_{(v,1)} = 112{,}73$ Btu/lbm

Similiarly, $P_{(l,3)} = 19.4$ psia

$h_{(l,3)} = 26.52$ Btu/lbm

(C) $h_{(v,2)} = h_{(v,1)} - L(h_{(v,2)} - h_{(v,3)})$

$h_{(v,2)} = 112.73 - .213(112.73 - 102.72) = 110.60$

From tables, $T_{(v,2)} = 158.6^\circ F.$

$P_{(v,2)} = 59.3$ psia

(D) $W_e = (E_e)(h_{(v,1)} - h_{(v,3)})(G) =$

$(.198)(112.73 - 102.72)(1800) = 1.05$ kw

(E) $p \approx 80$ psia

(F) $h_4 = h_3 + .373$ kw/1000 lbm $= h_3 + .707$ Btu/lbm $= 27.23$

$$T_4 - T_3 = \frac{.373 \text{ kw} - v(P_2 - P_1)}{c_v} = \frac{(.373 - .0648) \text{ kw}}{.21 \text{ Btu/lbm}^\circ\text{F}} =$$

2.78°F.

$T_4 = 92.3^\circ$F

The predicted system performance for $T_{boiler} = 210^\circ$F., $T_{condenser} = 60^\circ$F., and G= 35 lbm/min, using the preceeding procedure, is:

(A) Assuming $Q_e = 180{,}000$ Btu's/hr.

$T_e = 180{,}000/4884 = 36.9^\circ$F.

$T_c = 174{,}000/5100 = 34.1^\circ$F.

$T_{(v,1)} = 210 - 36.9 = 173.1^\circ$F.

$T_{(l,1)} = 60 + 34.1 = 94.1^\circ$F.

$Q_e = (h_{(v,173.1)} - h_{(l,94.1)})(G) =$

$(112.17 - 27.47)(2100) = 177{,}878$ Btu/hr

To a 2nd approximation

$T_e = 177{,}878/4884 = 36.4^\circ$F.

$T_c = 169{,}370/5100 = 33{,}3^\circ$F.

$T_{(v,1)} = 210 - 36.4 = 173.6^\circ$F.

$T_{(l,3)} = 60 + 33.2 = 93.2^\circ$F.

(B) From tables,

$P_{(v,1)} = 72.9$ psia

$h_{(v,1)} = 112.23$

Similiarly, $P_{(l,3)} = 32.9$ psia

$h_{(1,3)} = 27.28$ Btu/lbm

(C) $h_{(v,2)} = h_{(v,1)} - L(h_{(v,1)} - h_{(v,3)})$

$h_{(v,2)} = 112.23 - .362(112.23 - 103.14) =$

108.94 Btu/lbm.

From tables,

$T_{(v,2)} = 143.6$ F.

$P_{(v,2)} = 32.9$ psia

(D) $W_e = (E_e)(h_{(v,1)} - h_{(v,3)})(G) =$

$(.302)(112.23 - 103.14)(2100) = 1.69$ kw

(E) $p \approx 80$ psia

(F) $h_4 = h_3 + .373$ kw/2100 lbm $= h_3 + .606$ Btu/lbm $=$

27.89 Btu/lbm

$$T_4 - T_3 = \frac{(.373 - .0762)\text{kw}}{.21 \text{ Btu/lbm F}} = 2.30^\circ\text{F}.$$

$T_4 = T_3 + 2.30 = 95.5^\circ$F.

References

1. "Air Motors." Machine Design. September 12,1974, p. 216-218.

2. Barber, Robert E. "Solar Air Conditioning Systems Using Rankine Power Cycles-Design and Test Results of Prototype Three Ton Unit." Presented at the Institute of Environmental Sciences' 1975 Annual Meeting, April, 1975, in Los Angeles, California.

3. Cravalko, Ernest G., and Joseph L. Smith, Jr. Thermodynamics. Holt, Rinehart, and Winston. p. 6.15.

4. Eckard, Sprugeon E. "Multi-vane Expander as Prime Mover in Low temperature Solar or Waste Heat Application." IECEC '75 Record, p. 1399-1405. No. 759204.

5. Eckard, Spurgeon E. and James A. Bond."Performance Characteristics of a 3-Ton Rankine Powered Vapor-Compression Air-Conditioner," Presented at the Workshop on the Use of Solar Energy for the Cooling of of Buildings, UCLA Extension, University of California, Los Angeles, August 4-6, 1975.

6. Faires, Virgil M. Thermodynamics. (MacMillan

Publishing Co., Inc.: New York). 1970. p. 65,119.

7. Fraas, Arthur P. Heat Exchanger Design. (John Wiley and Sons, Inc.: New York). 1965. p. 206.

8. Gunther, R. Refrigeration, Air Conditioning, and Cold Storage. (Chilton Book Co., Philadelphia). 1969. p. 806-807.

9. Lindsley, E. F. "Wally Minto's Wonder Wheel." Popular Science. March 1976. p. 79.

10. Robertson, Gerald F., and Carl H. Wolgemuth. "Analysis and Test Apparatus for a Vane Expander Using Steam." IECEC '75 Record, p. 1406-1410. No. 759205.

11. Rohsenow, Warren M., and Harry Choi. Heat, Mass, and Momentum Transfer. (Prentice-Hall, Inc.: Englewood Cliffs). 1961.

12. ASHRAE Thermodynamic Properties of Refrigerants. (American Society of Heating, Refrigerating, and Air-Conditioning Engineers, Inc.: New York). p. 8-15, 313-314.

13. Correspondence between S. E. Eckard and myself. July 19, 1976.

14. Correspondence between myself and a refrigerator repairman.